Measurement of the Excitation Functions in Alpha-induced Reactions on ^{93}Nb from Threshold Energy to 39.5 MeV

Muhammad Shahid, Kwangsoo Kim, Guinyun Kim,* Muhammad Zaman and Muhammad Nadeem

Department of Physics, Kyungpook National University, Daegu 41566, Korea

Haladhara Naik

Radiochemistry Division, Bhabha Atomic Research Centre, Mumbai 400085, India

Mansoureh Tatari

Yazd University, Faculty of Physics, University of Yazd, Yazd 89195-741, Iran

R. Guin and S. K. Das

Radiochemistry Division, Bhabha Atomic Research Centre,
Variable Energy Cyclotron Centre, 1/AF Bidhan Nagar, Kolkata-700064, India

(Received 26 January 2015, in final form 15 July 2015)

The excitation functions of ^{93m}Mo and ^{91m,92m,95m,g}Nb produced from alpha-induced reactions on ^{93}Nb were measured from their respective threshold to 39.5 MeV. The study was conducted using the alpha beam from the Variable Energy Cyclotron Centre (VECC), Kolkata, India, the stacked foil activation technique and the off-line gamma ray spectrometric technique. The integral yields for a thick target were also deduced from the measured cross-sections and the stopping power of niobium. The results were compared with earlier reported data as well as with the theoretical values obtained from the TENDL-2013 library based on the TALYS-1.6 code.

I. INTRODUCTION

The demand for charged particle induced nuclear reactions to measure the excitation functions is increasing due to a wide range applications. The study of charged particle activation supports the validation of theoretical models of nuclear reactions, the optimization of the production of radionuclides, and the description of the nuclear processes during interactions of primary cosmic rays with extraterrestrial matter. The use of radioisotopes is significant in modern medical and research practices. Neutron-rich radioisotopes produced by using reactors and neutron-deficient radioisotopes produced by cyclotrons decay with specific modes and fulfil specific medical needs. Although multiple radioisotopes are now available to fulfil the requirements, still some compromises are necessary, and the spectra of radioisotopes are not complete. A number of tumors sites where radioisotopes are not effective are still treated conventionally.

Currently, the efforts are being made to identify the radioisotopes that can be delivered selectively with minimum side effects and to introduce pain & tumor progression reducing radioisotopes. That's why research on easy production and effective application of the radioisotopes is ongoing [1–3].

Only a limited number of excitation functions for alpha-induced reactions on 93Nb are available in various energy ranges [4–16]. In the present work, we measured the excitation functions of ^{93m}Mo and ^{91m,92m,95m,95g}Nb from the ^{93}Nb(α,x) reactions by using stacked foil activation and an off-line γ-ray spectrometric technique in the energy range of their respective reaction threshold up to 39.5 MeV at Variable Energy Cyclotron Centre (VECC), Kolkata, India. The detection efficiency of the detector as a function of the photon energy was determined at a 1 to 12 cm distance from the end-cap of the detector to avoid coincidence losses, and to assure a low dead time ($< 10\%$) and a point-like geometry. The production of ^{93m,g,94m,g,95m,g}Tc was also identified but the results will be reported in a separate publication. The

*E-mail: gnkim@knu.ac.kr; Fax: +82-53-939-3972

Table 1. Decay data of the radionuclides from the ^{93}Nb(α,x) and ^{nat}Cu(α,x) reactions. Gamma ray energies shown were used in the cross-section calculations.

Nuclide	Half-life $T_{1/2}$	Gamma Energy E_γ (keV)	Gamma Intensity I_γ (%)	Nuclear reaction	Decay mode (%)	Q-value (MeV)	Threshold Value E_{th} (MeV)
^{66}Ga	9.49 h	1039.2	37	^{63}Cu(α,n)	EC(43.19); β^+ (56.81)	-7.50	7.98
				^{65}Cu(α,3n)		-25.33	26.89
^{67}Ga	3.2617 d	184.6	21.41	^{63}Cu(α,γ)	EC(100)	3.72	0.000
		300.2	16.64	^{65}Cu(α,2n)		-14.10	14.97
^{65}Zn	243.93 d	1115.5	50.04	^{63}Cu(α,d)	EC(98.58); β^+ (1.42)	-10.38	11.04
				^{63}Cu(α,np)		-12.60	13.40
				^{65}Cu(α,nt)		-21.95	23.30
				^{65}Cu(α,2nd)		-28.20	29.94
				^{65}Cu(α,3np)		-30.43	32.30
^{93m}Mo	6.85 h	263.1	57.4	^{93}Nb(α,nt)	IT(99.88); EC(0.12)	-21.00	21.91
		684.7	99.9	^{93}Nb(α,2nd)		-27.26	28.43
		1477.1	99.1	^{93}Nb(α,3np)		-29.48	30.75
^{91m}Nb	60.86 d	104.6	0.58	^{93}Nb(α,α2n)	IT(96.6); EC(3.399); β^+(0.001)	-16.72	17.44
		1204.7	2.0	^{93}Nb(α,2t)		-28.05	29.26
				^{93}Nb(α,ndt)		-34.31	35.78
				^{93}Nb(α,2npt)		-36.53	38.10
^{92m}Nb	10.15 d	934.4	99.15	^{93}Nb(α,αn)	EC(99.993); β^+ (0.007)	-8.83	9.21
				^{93}Nb(α,dt)		-26.42	27.56
				^{93}Nb(α,npt)		-28.64	29.88
				^{93}Nb(α,2n^{3}He)		-29.41	30.68
				^{93}Nb(α,n2d)		-32.68	34.08
				^{93}Nb(α,2npd)		-34.90	36.40
^{95m}Nb	3.61 d	235.7	24.8	^{93}Nb(α,2p)	IT(94.4); β^- (5.6)	-12.58	13.12
^{95g}Nb	34.991 d	765.8	99.81	^{93}Nb(α,2p)	β^- (100)	-12.58	13.12

experimental results for ^{93m}Mo and ^{91m,92m,95m,95g}Nb measured in this work were compared with the literature data [4–16] and the theoretical values obtained from the TENDL-2013 library [17] based on the computer code TALYS-1.6 [18]. The integral yields for thick targets of the investigated radioisotopes were calculated by using the excitation function and the electronic stopping power.

II. EXPERIMENTAL DETAILS AND DATA ANALYSIS

The production cross-sections for the reactions ^{93}Nb(α,x) at the i-th sample were determined by using the well-known activation formula [19]

$$\sigma(E_i) = \frac{\lambda C(E_i)}{\varepsilon(E_i) I_\gamma \rho t \varphi (1 - e^{-\lambda t_m}) e^{-\lambda t_c} (1 - e^{-\lambda t_{irr}})}, \quad (1)$$

where λ is the decay constant (sec^{-1}), $C(E_i)$ is the net counts under the photopeak for the i-th sample, $\varepsilon(E_i)$ is

the detection efficiency of the HPGe detector, I_γ is the γ-ray intensity, ρ is the atomic density, t is the target foils thickness (cm), ϕ is the proton beam's intensity (particles per sec), t_c is the cooling time (s), t_m is the counting time (s), and t_{irr} is the irradiation time (s). The decay data, such as the half-life ($T_{1/2} = \ln2/\lambda$), the γ-ray emission probability (I_γ) and the γ-ray energy (E_γ), used for identifying the produced radionuclide were taken from the Table of Radioactive Isotopes [20] and are given in Table 1. The Q-values and the threshold energies calculated on the basis of the atomic mass evaluation by Wang *et al.* [21] combined with the Q-value calculator [22] are also presented. The excitation functions of residual radioisotopes in the alpha-induced reactions of niobium metallic foils were measured as a functions of the alpha energy from their respective thresholds up to 39.5 MeV by using a stacked foil activation technique combined with off-line gamma spectrometry. The stacked foil activation technique, the activity determination, and the data evaluation procedures are described elsewhere [23–30]. Some important features relevant to the present
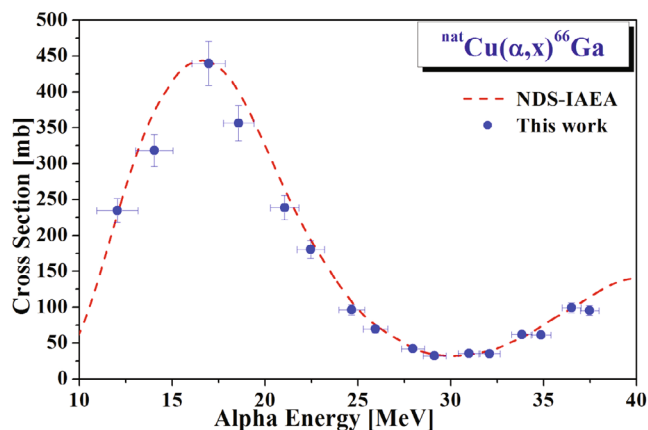
Fig. 1. (Color online) Excitation function of the $^{nat}Cu(\alpha,x)^{66}Ga$ reaction compared with the NDS-IAEA recommended data.

Fig. 2. (Color online) Excitation function of the $^{nat}Cu(\alpha,x)^{67}Ga$ reaction compared with the NDS-IAEA recommended data.

Fig. 3. (Color online) Excitation function of the $^{nat}Cu(\alpha,x)^{65}Zn$ reaction compared with the NDS-IAEA recommended data.

work are described below.

A high-purity (99.9%) niobium foil (17.5-μm thickness) with a size of 1.0 cm $\times$ 1.0 cm was used as a target material. Natural copper foils (> 99% purity, 10-μm thickness) with a size of 1.0 cm $\times$ 1.0 cm were used as flux monitors and energy degraders. The sequence of niobium and copper foils in a stack was designed on the basis of the threshold values for the products from the $^{93}Nb(\alpha,x)$ and the $^{nat}Cu(\alpha,x)$ reactions. The purpose of multiple monitor foils within the alpha energy range of $17.8 - 38.0$ MeV was to decrease unknown systematic errors in the activity measurements. The alpha energy degradation along the stacked foils was estimated by using the computer program SRIM-2013 [31]. The estimated average energy losses in the monitor and the sample foils were in the range of $0.51 - 1.11$ MeV and $0.75 - 1.22$ MeV, respectively. In this work, the entire study included the activation of two stacks in two different experiments under the same irradiation setup. In the first experiment, the stack was composed of 8 sets of {Nb-Cu} foils followed by one set of {Nb-Nb-Nb} foils. In the 2nd experiment, the foil sequence was exactly the same except for the addition of a 25-μm-thick Al foil that was positioned in the front of the stack and the removal of one of the three Nb foils at the end. This additional foil was associated with alpha energy loss; consequently, it provided an energy shift to the subsequent foils in the stack.

In the first experiment, the stack was irradiated by using a 39.5-MeV alpha beam, 120 nA beam current collimated to 10 mm in diameter for 45 min in the external beam line of the VECC, Kolkata, India [32]. In the second experiment, the beam energy and diameter were exactly the same; however, the beam current was 60 nA, and the irradiation time was 90 min. The experimental conditions and the irradiation geometry were kept constant during the irradiation for the two experiments. The stack was aligned with the beam so that the
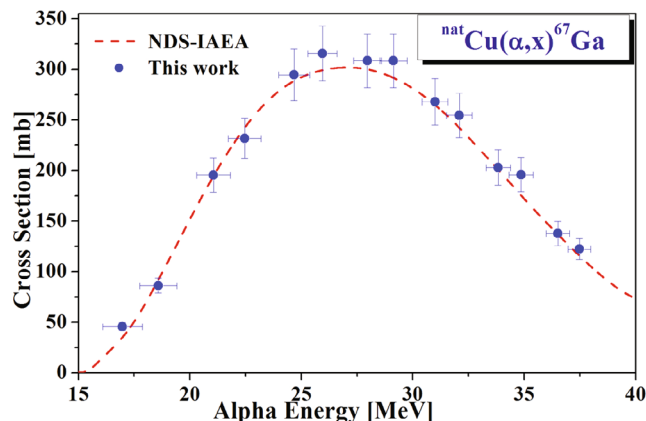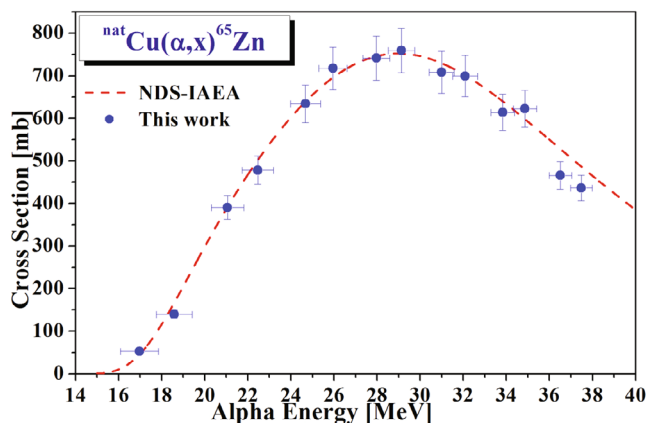
foils in the sample get the maximum exposure. After irradiation and an appropriate cooling time, the irradiated foils were removed and measured by using an n-type coaxial HPGe γ-ray spectrometer coupled to a PC-based 4096-channel analyzer with the associated electronics to determine the photopeak area of the γ-ray spectrum by using the Gamma vision 5.0 (EG&G Ortec) program.

The energy resolution of the detector was 1.9-keV full width at half maximum (FWHM) at the 1332.5-keV γ-ray photopeak of ^{60}Co. The photopeak efficiency curve of the γ-ray spectrometer was determined at different distances by using the standard gamma source ^{152}Eu having γ-rays in the energies range of $121.8 - 1408.0$ keV. The activity measurements of the irradiated samples were started after $2 - 3$ hours from the end of the bombardment (EOB). The measurements of the activated targets and the monitor foils were repeated several times for up to 15.7 days to follow the decay of the radionuclides and thereby to identify possible interfering nuclides. The alpha-beam's intensity and energy

Table 2. Cross-sections for the production of ^{66,67}Ga and ^{65}Zn radioisotopes by the ^{nat}Cu(α,x) reaction and of ^{93m}Mo, ^{91m,92m,95m,95g}Nb radioisotopes by the ^{93}Nb(α,x) reaction.

Monitor Reaction Products			
Alpha Energy	Cross-section (mb)		
(MeV)	^{66}Ga	^{67}Ga	^{65}Zn
37.49 ± 0.51	95.19 ± 6.89	122.43 ± 10.51	436.77 ± 30.19
36.51 ± 0.52	99.18 ± 7.02	137.87 ± 11.92	465.80 ± 32.56
34.86 ± 0.54	61.04 ± 4.55	195.72 ± 16.79	622.24 ± 42.90
33.83 ± 0.55	61.79 ± 4.43	202.93 ± 17.46	614.02 ± 42.84
32.09 ± 0.58	35.28 ± 2.78	254.54 ± 21.84	699.47 ± 48.20
31.00 ± 0.58	35.45 ± 2.61	268.06 ± 23.06	708.39 ± 49.38
29.13 ± 0.62	32.05 ± 2.56	308.52 ± 26.47	759.38 ± 52.31
27.96 ± 0.62	42.08 ± 3.07	308.70 ± 26.55	741.38 ± 51.66
25.95 ± 0.66	69.62 ± 5.15	315.85 ± 27.10	717.58 ± 49.44
24.68 ± 0.69	96.08 ± 6.81	294.65 ± 25.35	634.13 ± 44.23
22.47 ± 0.73	180.28 ± 12.75	231.80 ± 19.89	478.41 ± 33.04
21.06 ± 0.76	238.69 ± 16.70	195.43 ± 16.82	390.49 ± 27.35
18.58 ± 0.83	356.56 ± 24.84	86.27 ± 7.41	139.83 ± 9.83
16.97 ± 0.89	439.65 ± 30.63	45.69 ± 3.95	52.97 ± 3.95
14.04 ± 1.01	318.36 ± 22.22		
12.06 ± 1.11	234.80 ± 16.43		

^{93}Nb(α,x) Reaction Products					
Alpha Energy	Cross-section (mb)				
(MeV)	^{93m}Mo	^{91m}Nb	^{92m}Nb	^{95m}Nb	^{95g}Nb
38.75 ± 0.75	2.33 ± 0.23	17.42 ± 2.44	16.78 ± 1.16	0.13 ± 0.014	2.92 ± 0.21
37.79 ± 0.76	1.78 ± 0.17	14.05 ± 2.37	16.43 ± 1.15	0.06 ± 0.012	2.55 ± 0.19
36.19 ± 0.79	0.79 ± 0.08	11.56 ± 1.90	16.48 ± 1.14	0.09 ± 0.010	2.60 ± 0.19
35.18 ± 0.80	0.57 ± 0.09	7.05 ± 1.58	15.40 ± 1.08	0.09 ± 0.015	2.55 ± 0.19
33.49 ± 0.83		2.66 ± 0.83	14.65 ± 1.01	0.01 ± 0.004	1.94 ± 0.15
32.43 ± 0.85		0.90 ± 0.64	13.73 ± 0.96		1.53 ± 0.12
30.63 ± 0.88			13.63 ± 0.94	0.01 ± 0.007	0.93 ± 0.08
29.50 ± 0.91			12.25 ± 0.86		0.56 ± 0.05
27.56 ± 0.95			9.40 ± 0.65		
26.36 ± 0.99			6.58 ± 0.47		
24.25 ± 1.05			4.73 ± 0.33		
22.90 ± 1.08			3.12 ± 0.23		
20.57 ± 1.16			0.32 ± 0.03		
19.08 ± 1.22			0.04 ± 0.01		
19.08 ± 1.22					
19.08 ± 1.22					

were estimated by using the three monitor reactions, ^{nat}Cu(α,x)^{65}Zn, ^{nat}Cu(α,x)^{66}Ga and ^{nat}Cu(α,x)^{67}Ga, recommended by the IAEA [33]. The excitations functions of ^{66,67}Ga and ^{65}Zn were determined by using the measured beam intensities in the two experiments. The results are graphically presented in Figs. 1 − 3 in comparison with the standard NDS-IAEA values [33] and are

in good agreement with the recommended data points.

The uncertainty of the alpha energy for each representive energy point in the stack depends on the irradiation circumstances and the position of the foil in the stack. These are due to the initial beam energy, the thickness and homogeneity of target foils, and the beam straggling. The estimated uncertainty of a representing point in the
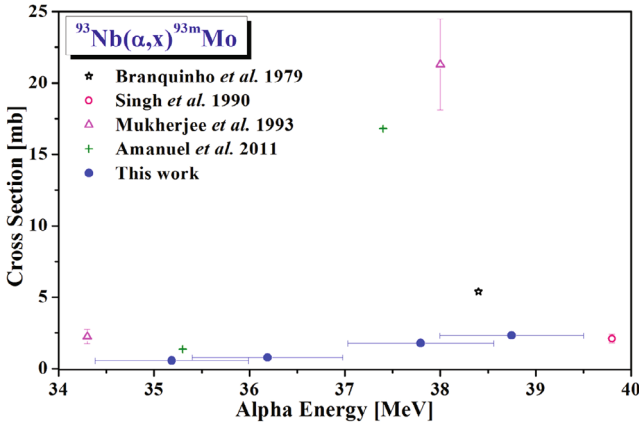
Fig. 4. (Color online) Excitation function of the ^{93}Nb$(\alpha,$x$)^{93m}$Mo reaction compared with the reported experimental data [4, 8, 10, 16] as well as data obtained from the TENDL-2013 library based on the model code TALYS-1.6.
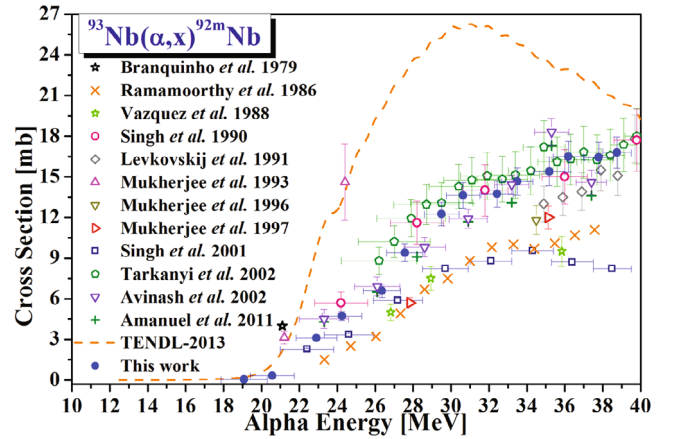
Fig. 6. (Color online) Excitation function of the ^{93}Nb$(\alpha,$x$)^{92m}$Nb reaction compared with the reported experimental data [4, 5, 7–16] as well as data obtained from the TENDL-2013 library based on the model code TALYS-1.6.
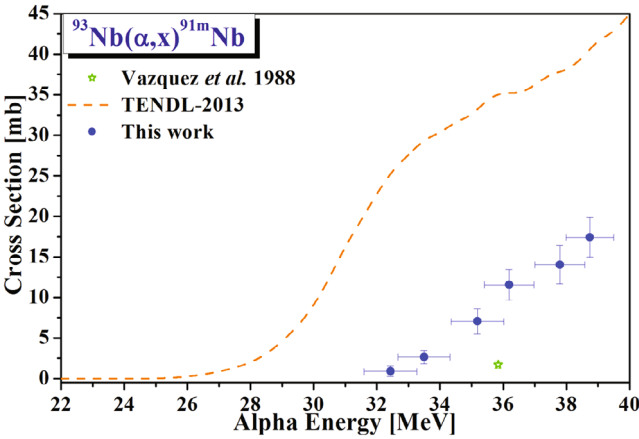
Fig. 5. (Color online) Excitation function of the ^{93}Nb$(\alpha,$x$)^{91m}$Nb reaction compared with the reported experimental data [7] as well as data obtained from the TENDL-2013 library based on the model code TALYS-1.6.
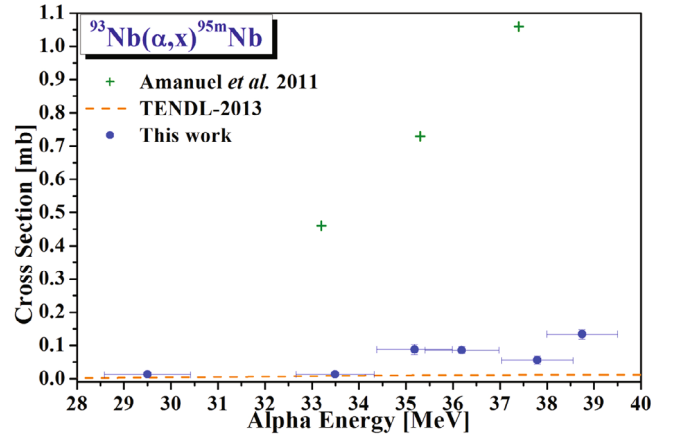
Fig. 7. (Color online) Excitation function of the ^{93}Nb$(\alpha,$x$)^{95m}$Nb reaction compared with the reported experimental data [16] as well as data obtained from the TENDL-2013 library based on the model code TALYS-1.6.

alpha energy range from ±0.75 to ±1.22 MeV are shown in Table 2 and Figs. 4 − 8.

Total uncertainties of the cross-sections were obtained according to the guidelines of error propagation or assuming that all uncertainties were independent. Moreover, some of the sources of uncertainties were common to all data while others affected each reaction or energy point individually. However, the combined uncertainty in each cross-section was estimated by considering the following uncertainties; statistical uncertainty of the γ-ray counting (6% ∼ 24%), of the alpha-beam's intensity (5.20% ∼ 5.29%), of the efficiency calibration of the detector (3% ∼ 4%), due to the sample thickness (1% ∼ 2%), and of the gamma-ray's intensity (1% ∼ 2%). The overall uncertainties of the measured cross-sections were in the range of 8.60% ∼ 25.06%.

III. RESULTS AND DISCUSSION

The experimentally-determined independent and cumulative cross-sections for productions of radioisotopes of niobium and molybdenum by irradiation of ^{93}Nb with alpha particles were measured and are given in Table 2. The estimated uncertainties in the energy and the cross-section values are also presented. The data were plotted as functions of -particle energy and compared with the experimental data available in the EXFOR library [34] and with the theoretical data calculated with TALYS-1.6, as shown in Figs. 4 − 8. The details of the reaction and the products are given in subsections 1 − 4 below. The integral yields for thick targets were also determined by using the measured production cross-sections and the stopping power of ^{93}Nb over the energy region from threshold to the initial alpha energy, as shown in
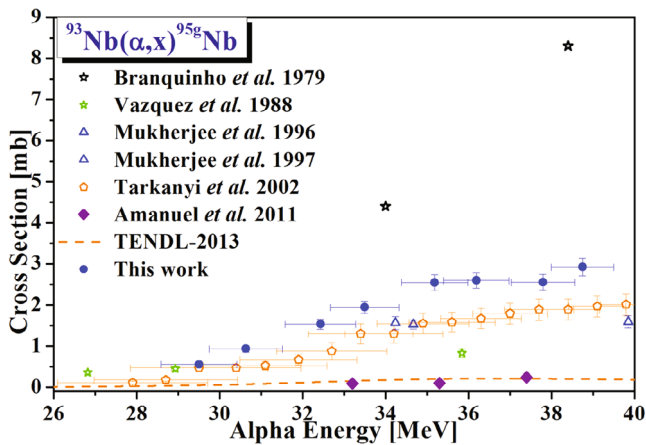
Fig. 8.   (Color online) Excitation function of the
^{93}Nb$(\alpha,x)^{95g}$Nb reaction compared with the reported exper-
imental data [7,11,12,17] as well as data obtained from the
TENDL-2013 library based on the model code TALYS-1.6.
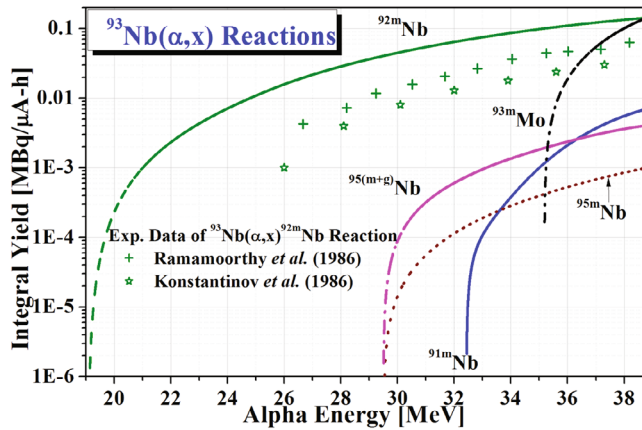
Fig. 9. (Color online) Integral yield for the production of
^{93m}Mo and ^{91m,92m,95m,95g}Nb radionuclides from ^{93}Nb(α,x)
reactions.

Fig. 9. The descriptions for thick-target yields are given
in subsection 5.

1. ^{93}Nb$(\alpha,x)^{93m}$Mo Reaction

The radionuclide ^{93}Mo is produced directly from the
^{93}Nb(α,x) reaction. Different reaction channels that
open at different thresholds contribute to the production
of this radionuclide. ^{93}Mo has a very long-lived ground
state ^{93g}Mo (T$_{1/2}$ = 4 × 10^3 y) and a relatively short
lived meta-stable state ^{93m}Mo (T$_{1/2}$ = 6.85 h). The
decay scheme reveals that ^{93m}Mo decays to ^{93g}Mo and
^{93}Nb through the IT mode (99.88%) and the EC process
(0.12%), respectively. The production of ^{93g}Mo was not
identified because it emits only one gamma line of 30.8
keV (I$_\gamma$ = 5.2 × 10^{-4}%), which could not be detected

with the current spectrometric setup. The gamma-ray
spectra taken after 2.54 hours of cooling were analyzed
to identify the production of ^{93m}Mo through its three
intense and interference-free γ-lines mentioned in Table
1. The measured cross-sections given in Table 2 are
averages of the values obtained with the three gamma
lines. The measured cross-sections for ^{93m}Mo together
with data from the literature [4,8,10,16] are presented
in Fig. 4. Currently, neither the TENDL-2013 library
nor the TALYS-1.6 code provides theoretical calcula-
tions for ^{93m}Mo. The comparison shows that the current
measurements are comparable to the experimental data
points; however, above 37 MeV, the results measured by
Mukherjee et al. [10] and Amanuel et al. [16] are higher
than the current measurements.

2. ^{93}Nb$(\alpha,x)^{91m}$Nb Reaction

The radionuclide ^{91}Nb is produced directly from the
contribution of different reaction channels with different
thresholds. ^{91}Nb has a long-lived ground state ^{91g}Nb
(T$_{1/2}$ = 680 y) and two meta-stable states, i.e., ^{91m1}Nb
(T$_{1/2}$ = 60.86 d) and ^{91m2}Nb (T$_{1/2}$ = 3.76 μs). The
activities of ^{91g}Nb and ^{91m2}Nb could not be identified
because ^{91g}Nb is not a gamma emitter while ^{91m2}Nb has
a very short half-life. The decay scheme reveals that
^{91m1}Nb decays to ^{91g}Nb by an IT process (96.6%) and
to stable ^{91}Zr by an EC process (3.4%). The radionu-
clide ^{91m1}Nb was identified in the gamma-ray spectra
taken after EOB+7.9 days by using the peak at 1204.6
keV (I$_\gamma$ = 2.0%). The measured cross-sections are given
in Table 2. The measured excitation functions, together
with the experimental data by Vázquez et al. [7] and the-
oretical values obtained from the TENDL-2013 library,
are shown in Fig. 5. The comparison shows that the lit-
erature data point is relatively lower than present data
while the theoretical calculations are over estimated.

3. ^{93}Nb$(\alpha,x)^{92m}$Nb Reaction

The radionuclide ^{92}Nb is directly produced through
the ^{93}Nb(α,x) reaction. The decay scheme reveals that
^{92}Nb has a very long-lived ground state ^{92g}Nb (T$_{1/2}$ =
3.47 × 10^7 y) and a meta-stable state ^{92m}Nb (T$_{1/2}$ =
10.15 d) that decay directly to the stable ^{92}Zr nuclide by
an EC process (100%). The production of ^{92g}Nb could
not be identified in the spectrum due to its long half-life.
The meta-stable state ^{92m}Nb was identified by its strong
and independent γ-line of 934.4 keV (I$_\gamma$ = 99.15%) in
the spectra that were taken after EOB+7.9 days. The
measured cross-sections for the ^{92m}Nb production, to-
gether with the literature data [4,5,7–16] and the theoret-
ical data from the TENDL-2013 library, are presented in

Fig. 6. The comparison shows that the measured cross-sections are comparable with the literature data Refs. [4,8,9] and [14–16], lower than the data in the Ref. [10] and higher than the data in the Refs. [5,7] and [11–13]. The literature data reveals that the theoretical model calculations are over estimated as compared with all experimental data.

4. ^{93}Nb(α,2p)^{95}Nb Reaction

The radionuclide ^{95}Nb is produced directly through the ^{93}Nb(α,2p) reaction, which is the only reaction channel with a threshold energy of 13.12 MeV. ^{95}Nb has a relatively long-lived ground state ^{95g}Nb (T$_{1/2}$ = 34.991 d) and a meta-stable state ^{95m}Nb (T$_{1/2}$ = 3.61 d). The decay scheme reveals that ^{95m}Nb decays to ^{95g}Nb and ^{95}Mo (stable) through an IT mode (94.4%) and a β^- mode (5.6%) respectively. The directly- and indirectly-produced ^{95g}Nb finally decays to ^{95}Mo through the β^- mode (100%) followed by the emission of one intense gamma ray. The spectra taken within EOB plus 7.9 − 15.7 days were analyzed to identify the production of ^{95m,g}Nb when the decay of ^{95m}Nb into ^{95g}Nb was more than 75% complete. The productions of ^{95m}Nb and ^{95g}Nb were identified with the most intense and interference-free gamma lines of 235.7 keV (I$_\gamma$ = 24.8%) and 765.8 keV (I$_\gamma$ = 99.81%), respectively. The contribution of ^{95m}Nb was subtracted in order to determine the direct production of ^{95g}Nb. The measured results for ^{95m}Nb and ^{95g}Nb are numerically given in Table 2 and graphically plotted, along with published data and theoretical values, in Figs. 7 and 8, respectively. Figure 7 shows that the current experimental data for ^{95m}Nb are higher than the theoretical values. The experimental data reported by Amanuel *et al.* [16] which are higher than the present measurements are the only data in the literature for this product. Figure 8 for ^{95g}Nb shows that the current experimental data are comparable to the data reported in Refs. [7, 11, 12, 14]; however, the data reported in Ref. [4] are higher and those reported in Ref. [16] are lower. Overall, theoretical model calculations are underestimated as compared with most of the reported experimental data points.

5. Integral Yields for Thick Target

The information on the integral yields for thick targets can be easily deduced from the production cross-sections of the radionuclides. The energy loss of the bombarding particles in a thin target is usually so small that any significant change in the reaction cross-sections throughout its thickness is hard to find. Therefore, a thick target is preferred to see this effect. The physical integral yields for thick targets [35] of the produced radioisotopes are determined from their measured excitation functions and the stopping power of ^{93}Nb over the energy region from threshold (E_{th}) to the initial alpha energy (E_{in}) by taking into account that the total energy is absorbed in the target. The physical integral yield is given by

$$Y = I_\alpha \cdot N_d \cdot \int_{E_{th}}^{E_{in}} \frac{\sigma(E)}{(dE/dx)_E} dE \times \lambda, \qquad (2)$$

where I_α is the number of incident α-particles per a constant charge equivalent to 1 μA $\times$ 1 h, N_d is the number density of the target material (atoms/cm^3), σ(E) is the measured excitation function (cm^2), $(dE/dx)_E$ is the stopping power of each target sample (MeV/cm), dE is the energy difference between two successive target (MeV), and λ (= ln $2/T_{1/2}$) is the decay constant of the produced radionuclide (sec^{-1}). The integral yield was finally obtained in unit of Bq/μA·h which can be converted to MBq/μA·h. The determined integral yields for the ^{93m}Mo and ^{91m,92m,95m,95g}Nb radionuclides are shown in Fig. 9 as functions of the alpha energy. Currently, the literature data [5,6] for ^{92m}Nb are available to compare with the measured yield. The comparison shows that the measured results in this work are higher than the reported values.

IV. CONCLUSION

We have measured the production cross-sections of the ^{93m}Mo and the ^{91m,92m,95m,95g}Nb radionuclides from ^{93}Nb(α,x) nuclear reactions in the energy region from their threshold energy to the maximum alpha energy with overall uncertainties in the range of 8.60% ∼ 25.06% by using a stacked foil activation method. We compared the present results with the experimental data available in literature and the data obtained from TENDL-2013 based on the computer code TALYS-1.6. Most of the present results find good agreement with the available experimental data. The integral yields of thick targets for the investigated radionuclides were also deduced from the measured excitation functions. The current experimental work is helpful in making the literature data more reliable and in modifying theoretical models.

ACKNOWLEDGMENTS

REFERENCES

[1] M. S. Uddin, M. U. Khandaker, K. S. Kim, Y. S. Lee and G. N. Kim, Nucl. Instr. Meth. B **258**, 313 (2007).

[2] M. U. Khandaker, M. S. Uddin, K. S. Kim, Y. S. Lee and G. N. Kim, Nucl. Instr. Meth. B **262**, 171 (2007).

[3] M. U. Khandaker, K. Kim, M. W. Lee, K. S. Kim, G. N. Kim, Y. S. Cho and Y. O. Lee, Appl. Radiat. Isot. **67**, 1341 (2009).

[4] C. L. Branquinho, S. M. A. Hoffmann, G. W. A. Newton, V. J. Robinson, I. S. Grant and J. A. B. Goodall, J. Inorg. Nucl. Chem. **41**, 791 (1979).

[5] N. Ramamoorthy, M. K. Das, B. R. Sarkar and R. S. Mani, J. Radioanal. Nucl. Chem. **98**, 121 (1986).

[6] I. Konstantinov, P. P. Dmitriev and V. I. Bolotskikh, J. SJA **60**, 390 (1986).

[7] M. E. Vázquez, M. J. Ozafrán, M. de la Vega Vedoya and S. J. Nassiff, J. Radioanal. Nucl. Chem. **121**, 203 (1988).

[8] N. L. Singh, A. Agarwal and J. Rama Rao, J. Phys. Soc. Jpn. **59**, 3916 (1990).

[9] V. N. Levkovskij, *Activation cross-section nuclides of average masses (A=40-100) by protons and alpha-particles with average energies (E=10-50 MeV)*, (Inter Vesi, Moscow, 1991).

[10] S. Mukherjee, M. H. Rashid and S. N. Chintalapudi, Pramana **41**, 329 (1993).

[11] S. Mukherjee and N. L. Singh, Nucl. Part. Phys. **22**, 1455 (1996).

[12] S. Mukhejee, N. L. Singh, A. V. Mohan Rao, L. Chaturvedi and P. P. Singh, Physica Scripta. **55**, 409 (1997).

[13] R. K. Y. Singh, M. A. Ansari and R. P. Gautam, Chinese J. Phys. **39**, 336 (2001).

[14] F. Tárkányi, F. Ditrói, F. Szelecsényi, M. Sonck and A. Hermanne, Nucl. Instr. Meth. B **198**, 11 (2002).

[15] A. Agarwal, I. A. Rizvi and A. K. Chaubey, Phys. Rev. C **65**, 034605 (2002).

[16] F. K. Amanuel, B. Zelalem, A. K. Chaubey, A. Agarwal and I. A. Rizvi, Chinese J. Phys. **49**, 884 (2011).

[17] A. J. Koning *et al.*, *TENDL-2013: TALYS-based evaluated nuclear data library, Nuclear Research and Consultancy Group (NRG)* (Petten, Netherlands, December 23, 2013), Available from: <ftp://ftp.nrg.eu/pub/www/talys/tendl2013/tendl2013.html>.

[18] A. J. Koning *et al.*, *Proceedings of the International Conference on Nuclear Data for Science and Technology* (EDP Science, Nice, France, 2008), p. 211, (April 22-27, 2007, Available from: <http://www.talys.eu>).

[19] G. Gilmore and J. D. Hemingway, *Practical Gamma-Ray Spectrometry* (John Wiley and Sons, England, 1995), Chap. 1, p. 17.

[20] National Nuclear Data Center, Brookhaven National Laboratory, information extracted from the NuDat 2 database (Available from: <http://www.nndc.bnl.gov/nudat2/>).

[21] M. Wang, G. Audi, A. H. Wapstra, F. G. Kondev, M. MacCormick, X. Xu and B. Pfeiffer, Chinese Phys. C **36**, 1603 (2012).

[22] National Nuclear Data Center, Brookhaven National Laboratory, Q-value Calculator (Available from: <http://www.nndc.bnl.gov/qcalc/>).

[23] M. U. Khandaker, K. Kim, M. W. Lee, K. S. Kim, G. N. Kim, Y. S. Cho and Y. O. Lee, Nucl. Instr. Meth. B **266**, 4877 (2008).

[24] M. U. Khandaker, K. Kim, K.-S. Kim, M. W. Lee, G. N. Kim, Y. S. Cho and Y. O. Lee, Nucl. Instr. Meth. B **266**, 5101 (2008).

[25] M. U. Khandaker, K. Kim, K. -S. Kim, M. W. Lee, Y. S. Lee, G. N. Kim, Y.-S. Cho and Y.-O. Lee, Nucl. Instr. Meth. B **267**, 23 (2009).

[26] M. U. Khandaker, K. S. Kim, G. N. Kim and N. Otuka, Nucl. Instr. Meth. B **268**, 2303 (2010).

[27] M. U. Khandaker, K. S. Kim, M. W. Lee, K.-S. Kim and G. N. Kim, Nucl. Instr. Meth. B **269**, 1140 (2011).

[28] M. U. Khandaker, K. S. Kim, M. W. Lee, K.-S. Kim, G. N. Kim and N. Otuka, Nucl. Instr. Meth. B **271**, 72 (2012).

[29] M. U. Khandaker, H. Haba, J. Kanaya and N. Otuka, Nucl. Instr. Meth. B **296**, 14 (2013).

[30] M. Shahid, K. Kim, H. Naik and G. N. Kim, Nucl. Instr. Meth. B **322**, 13 (2014).

[31] J. F. Ziegler, Nucl. Instr. Meth. B *219-220*, 1027 (2004). (Available from: <http://www.srim.org/>).

[32] S. Saha, J. Choudhury, G. Pal, D. P. Hajra, R. Dey, A. Sur and R. K. Bhandari, Cryogenics **49**, 235 (2009).

[33] S. M. Qaim *et al.*, *Charged Particle Cross-section Database for Medical Radioisotope Production: Diagnostic Radioisotopes and Monitor Reactions*, IAEA-TECDOC-1211 (Vienna, 2001). Available from: <https://www-nds.iaea.org/medical/>.

[34] National Nuclear Data Center, Brookhaven National Laboratory, EXFOR database (Available from: https://www-nds.iaea.org/exfor/exfor.htm).

[35] S. M. Qaim *et al.*, IAEA-TECDOC-1211 (Vienna, 2001). Available from: <https://www-nds.iaea.org/medical/definitions.pdf>.